

Investigation of Lightning and Storm Electrification Processes Using a Phased Array Radar and Lightning Mapping Array

CORY SCHULTZ*

*National Weather Center Research Experiences for Undergraduates Program
Norman, Oklahoma,
South Dakota Mines
Rapid City, SD*

DAVID SCHVARTZMAN AND DAVID BODINE

*School of Meteorology, University of Oklahoma
Advanced Radar Research Center, University of Oklahoma
Norman, Oklahoma*

VANNA CHMIELEWSKI

*NOAA / National Severe Storms Laboratory
Norman, Oklahoma*

TIAN-YOU YU

*Electrical and Computer Engineering, University of Oklahoma
Advanced Radar Research Center, University of Oklahoma
Norman, Oklahoma*

MICHAEL STOCK

*Cooperative Institute for Severe and High-Impact Weather Research and Operations, University of Oklahoma
NOAA / National Severe Storms Laboratory
Norman, Oklahoma*

ABSTRACT

Ice crystal alignment within thunderstorms is difficult to capture due to the temporal scale at which electrical build-up and breakdown occur. This study focuses on three principal objectives which include: determining how effective phased array radars (PARs) higher temporal resolution is at analyzing ice crystal alignment within thunderstorms, determining a correlation between Specific Differential Phase (K_{DP}) and Differential Reflectivity (Z_{DR}) signatures and the three-dimensional flash locations determined by a lightning mapping array (LMA), and finally, advancing our understanding of electrification signatures and how important the temporal scale is to the process. The fully digital polarimetric rotating S-band PAR system, Horus, conducted a series of range-height indicator (RHI) scans of a tornadic supercell on 11 May 2023 at 23:38 to 12 May 2023 at 00:56 UTC, within range of the Oklahoma LMA (OKLMA). Plotting these RHI scans along with the OKLMA data allowed for the examination of regions of negative K_{DP} or near-zero Z_{DR} values, which may correspond to vertical ice crystal alignment in large electric fields. In the end, Horus's K_{DP} signatures did not align with the lightning flashes in this case, but many flashes were in areas with near-zero Z_{DR} values. The storm was very electrified with 22,351 flashes occurring during the study period with 2,138 RHI scans, potentially beyond the point that 2-second RHI scans can capture storm electrification and the process of ice crystal alignment.

1. Introduction

The study of lightning has been ongoing for decades with past research investigating topics ranging from the number of flashes in a thunderstorm, to flash propagation, to

*Corresponding author address: Cory Schultz, South Dakota Mines,
501 E St Joseph St, Rapid City, SD 57701
E-mail: Cory.Schultz@mines.sdsmt.edu

the cloud microphysics that result in storm electrification (e.g., Maggio et al. 2005; Stough et al. 2022; Sullivan and Wells 1957). The storm electrification process depends on many different scales from the synoptic scale down to microscale, but one of the main factors contributing to this process is the storm's updraft. Storm electrification occurs due to the separation of charged particles in and around the updraft of thunderstorms where ideal conditions exist (Takahashi 1978). One of the consequences of storm electrification is the vertical alignment of ice crystals where electric fields are large (e.g., Biggerstaff et al. (2017)). However, this is not easily captured with the U.S. operational radars due to the slower scan times of the Weather Surveillance Radar - 1988 Doppler (WSR-88D) used by the National Weather Service (NWS). The WSR-88D scan times are on the order of 4-10 minutes per full-volume scan (Feng et al. 2009) while several lightning flashes can occur each second in an active thunderstorm (Hendry and Antar 1982). Ever-evolving electrification signatures require scan times faster than what the WSR-88D can provide, and newer generations of fast-scanning polarimetric radars can help improve the understanding of electrification phenomena.

Fast-scanning polarimetric radars are an important tool for the study of lightning and the associated cloud microphysics. With the introduction of the first phased array radar (PAR) dedicated to the observation of weather in 1997 (Maese et al. 2001), the use of PARs has come a long way since their conception in the early 1960s (Haupt and Rahmat-Samii 2015). PAR technology has drastically advanced since 1997 with the introduction of a fully digital polarimetric rotating S-band PAR system, Horus, which was developed at the Advanced Radar Research Center (ARRC) at the University of Oklahoma (OU), with support from the NOAA National Severe Storms Laboratory (NSSL). Horus, which is the first of its kind, has many advantages over other radars such as beam agility (on the order of microseconds), radar imaging (the ability to change the shape of the radar beam), adaptive scanning (most effective with PAR technology), and all-digital beamforming (software dependent, not hardware) (Palmer et al. 2023). These advantages allow Horus to conduct full-volume scans in 10-12 seconds at max rotation speed and collect range-height indicator (RHI) scans in less than 2 seconds. The temporal frequency of Horus scans may be fast enough to capture the build-up and breakdown of electric fields by the ice crystal signatures. By looking at the Specific Differential Phase (K_{DP}) from these RHI scans, the difference in orientation of the hydrometeors can be determined leading to the detection of vertically tilted hydrometeors (e.g., ice crystals) at higher elevations in the thunderstorm. Looking for regions of negative K_{DP} values (vertically oriented ice crystals) may be a promising way to determine the locations of strong electric fields (Biggerstaff et al. 2017). However, not all negative regions

of K_{DP} may be associated with ice crystal alignment, as the backscatter from conical graupel can also cause negative values (Zikmunda and Vali 1972). K_{DP} signatures may also be/not be present in locations where they are expected, either. A different approach to finding vertically oriented ice crystals is by looking at the Differential Reflectivity (Z_{DR}), which also indicates the preferred orientation of hydrometeors (Hubbert et al. 2014). However, there is still uncertainty when looking for the regions of storm electrification and ice crystal alignment using only radar scans. The potential for data artifacts is always present with radar data, potentially causing confusion in the interpretation and utilization of the data (Kumjian 2013).

To increase the certainty in which regions are associated with vertically oriented ice crystals in large electric fields, lightning mapping arrays (LMAs) can be integrated into the analysis. LMAs, which have been in use since 1998, monitor lightning in three spatial dimensions and time by using time-of-arrival geolocation of very high frequency (VHF) radiation sources due to electrical breakdown along lightning channels (Rison et al. 1999). They accurately track intracloud lightning flashes within thunderstorms that are within 200-300 km of multiple sensors (Chmielewski and Bruning 2016; Thomas et al. 2004). The Oklahoma LMA (OKLMA), first implemented in 2003 (MacGorman et al. 2008) and later expanded to the southwest in 2012 (Barth et al. 2015), has timing uncertainties that range from 38 to 45 ns rms (Root-Mean-Square) for VHF sources mapped by six or more stations (Thomas et al. 2004). Knowing when the flash happened and where in the cloud it was are both crucial for testing ice crystal alignment.

The combination of polarimetric radars and LMAs is a logical next step to further understand the storm electrification process and the microphysics that comes into play (Biggerstaff et al. 2017). During electrical discharge, electric fields and ice crystal alignments within them diminish rapidly but can rebuild in the same general area over a period of several seconds (Hendry and Antar 1982). It is crucial to obtain the highest temporal resolution possible to better capture evolution in ice crystal alignment signature and the correlated lightning flashes. Using Horus will increase this temporal resolution, allowing for a more detailed analysis of cloud microphysics, and potentially capturing a more complete picture of the cloud electrification and ice crystal alignment processes.

In this study, similar to the work done by Biggerstaff et al. (2017), RHI scans were conducted through a tornadic supercell, to capture the vertical structure of the storm and analyze the locations of negative K_{DP} . Where this study differs from previous studies of this type is the use of the Horus PAR. This study aims to address a series of issues regarding storm electrification research. These issues include, how effective PARs higher temporal resolution is at analyzing the ice crystal alignment within thunderstorms,

determining a correlation between such radar signatures and the three-dimensional flash locations, and finally, advancing our understanding of electrification signatures and how important the temporal scale is to that process.

2. Data and Methods

On 11 May 2023 from 23:38 to 12 May 2023 at 00:56 UTC, a tornadic supercell embedded in a small squall line was observed over central Oklahoma. Horus was deployed to 35.1864315°N and 97.445871°W to scan RHIs at azimuth angles set to 270°, 270°, and 285°. The beam width was set to a “pancake” beam, at about 12° in azimuth and 3.5° in elevation. The elevation angles were from 0.5° to 31.5° in increments of 0.5° (64 beams per RHI scan). The range resolution was 19.2 m, the first gate was set to 19.2 m, and the max range was 55 km. During the 1-hour and 18-minute time, 2,138 RHI scans were conducted at 2-second intervals.

At the time of the storm, 10 of the OKLMA sensors were operational, 9 of which were in the central Oklahoma cluster. For the entire duration of the operation, the storm was within three-dimensional mapping and high detection efficiency range and 22,351 unique flashes were detected.

The focus of this research occurred during the study period from 11 May 2023 at 23:38 to 12 May 2023 at 00:00 UTC, due to higher flash rate occurrences in and around the main updraft of the storm and higher flash counts per RHI scan over the whole scan period. To establish the area of interest regarding the Horus scans and the supercell, Oklahoma City’s WSR-88D (KTLX) base reflectivity was plotted to examine the relative RHI view through the storm. As for jointly displaying the Horus and LMA data, this required new code to be developed in Python using the Py-ART (Helmus and Collins 2016) and Pyxlm packages (<https://github.com/deeplycloudy/xlma-python>). K_{DP} was calculated using the Vulpiani method (Vulpiani et al. 2012) in Py-ART, then the -0.1 to 0.1 range was removed to mask noise around the scan perimeter. Z_{DR} values were also analyzed as another way to determine ice crystal orientation. The OKLMA data was filtered with a minimum station count of 6 per VHF source, a maximum reduced 2 value of 1.0, a maximum time difference of 2 seconds after the RHI scan, and a maximum distance from the RHI scan of 3 km. The `lmatools` method for flash-sorting was used to determine the number of flashes during a given RHI scan (Fuchs et al. 2016). For flash clustering, the VHF source criteria were the same with a maximum distance of 3 km and 0.15 seconds between sources, and a maximum flash duration of 3 seconds. And finally, a minimum number of 10 sources per flash per event was used, which may filter out some of the smaller flashes, but reduce uncertainties for plotting.

3. Results

Storm Overview and Radar Positions

On 11 May 2023 at 23:44:09 UTC, there was a small squall line system present with at least one tornadic supercell embedded in the line (Figure 1). The storm’s relative motion was NNE at roughly 29 knots. At this point in time, Horus was positioned at 35.1864315°N and 97.445871°W with an azimuth angle of 270° looking due west (see Figure 1 for position compared to KTLX). Strong reflectivity signatures were present throughout the squall line (mid-40s to low-50s dBZ) with isolated regions of higher reflectivity (mid-50s dBZ). By 23:57:02 UTC (Figure 2), most of the squall line had moved off to the North, leaving just the tail end of the main supercell to still be scanned by Horus.

Vertical Ice Crystal Alignment

From 11 May 2023 at 23:38:29 to 12 May 2023 at 00:00 UTC, regions of slightly negative K_{DP} values were present in the Horus RHI scans, potentially indicating vertical ice crystal alignment due to storm electrification. For example: at 23:38:29 UTC, there is a region of slightly negative K_{DP} that was located roughly 40 km from the radar and roughly 10 km in altitude within the supercell (Figure 3). This region of negative K_{DP} appears just above an area of higher reflectivity (50 dBZ) which is associated with the storm’s updraft. If we compare this to the following RHI scan at 23:38:31 UTC (Figure 4), the shape and location of the negative K_{DP} region are approximately the same with only minor deviation. Analyzing the rest of the RHI scans after this study period (not shown), this region of negative K_{DP} is prominent, with minor expansions, until roughly 23:41:00 UTC where the region starts to fluctuate, slowly switching between negative and positive K_{DP} values over the course of several scans. Comparing Figures 3 and 4, this is not the case, so we also analyzed the differential reflectivity (Z_{DR}) for regions of negative or near-zero values which would also indicate vertically orientated ice crystals or close to it. Looking at Figures 3 and 4, there are regions of near-zero Z_{DR} values above the updraft of the storm and in the same vicinity as the region of negative K_{DP} . These near-zero Z_{DR} values persist throughout the rest of the study period with varying locations and intensities (not shown).

Analyzing the OKLMA data along with the RHI scans provides validation as to where flashes occurred around the K_{DP} and Z_{DR} values. The location of the data plotted on the RHI in Figure 3 shows VHF sources in a region to the left (east) of the area of negative K_{DP} . Comparing this to Z_{DR} , the VHF sources are more in line with the locations of near-zero Z_{DR} values than the negative K_{DP} values for this RHI. Looking at Figure 4, some VHF sources

KTLX 23:44:09 UTC 11 May 2023 0.48 deg.

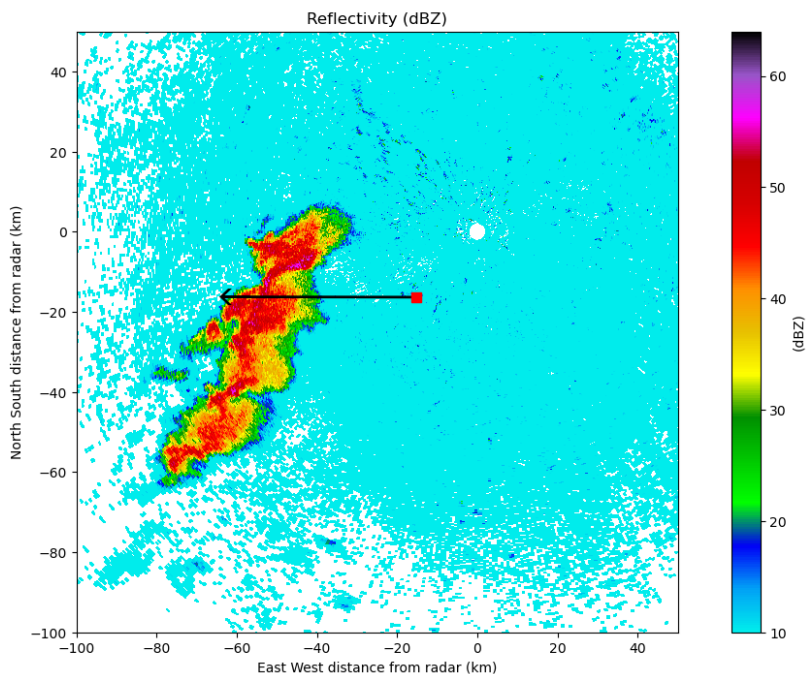


FIG. 1. Base (0.48° elevation) PPI scans of radar reflectivity (dBZ) from the Oklahoma City, OK, WSR-88D radar, KTLX, of a tornadic supercell embedded in a squall line on 11 May 2023 at 23:44:09 UTC. The red square is the location of the mobile PAR, Horus, scanning RHIs at a 270° azimuth angle (black line).

KTLX 23:57:02 UTC 11 May 2023 0.48 deg.

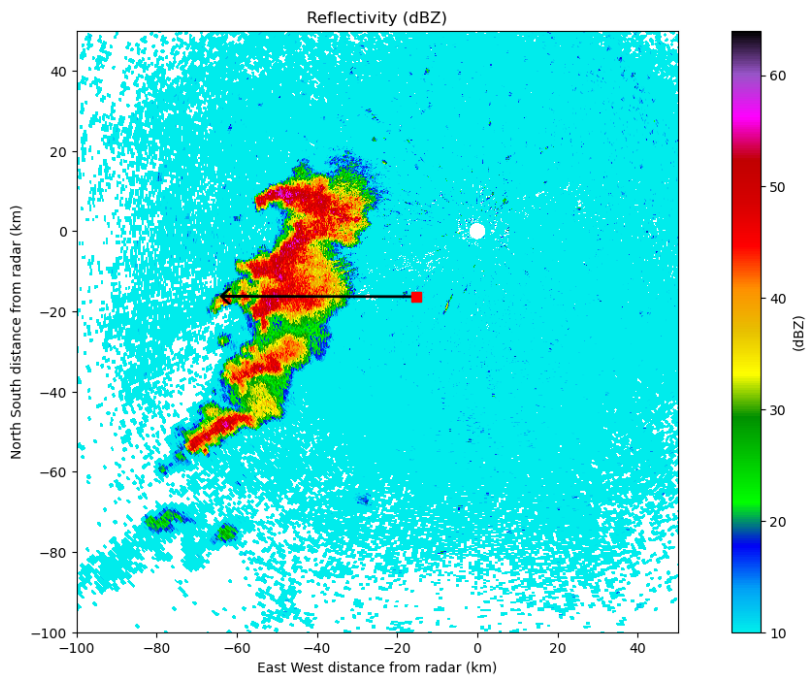


FIG. 2. Same as in Figure 1, but at 23:57:02 UTC, 12 minutes, and 53 seconds after Figure 1.

HRUS 2023-05-11 23:38:29 UTC

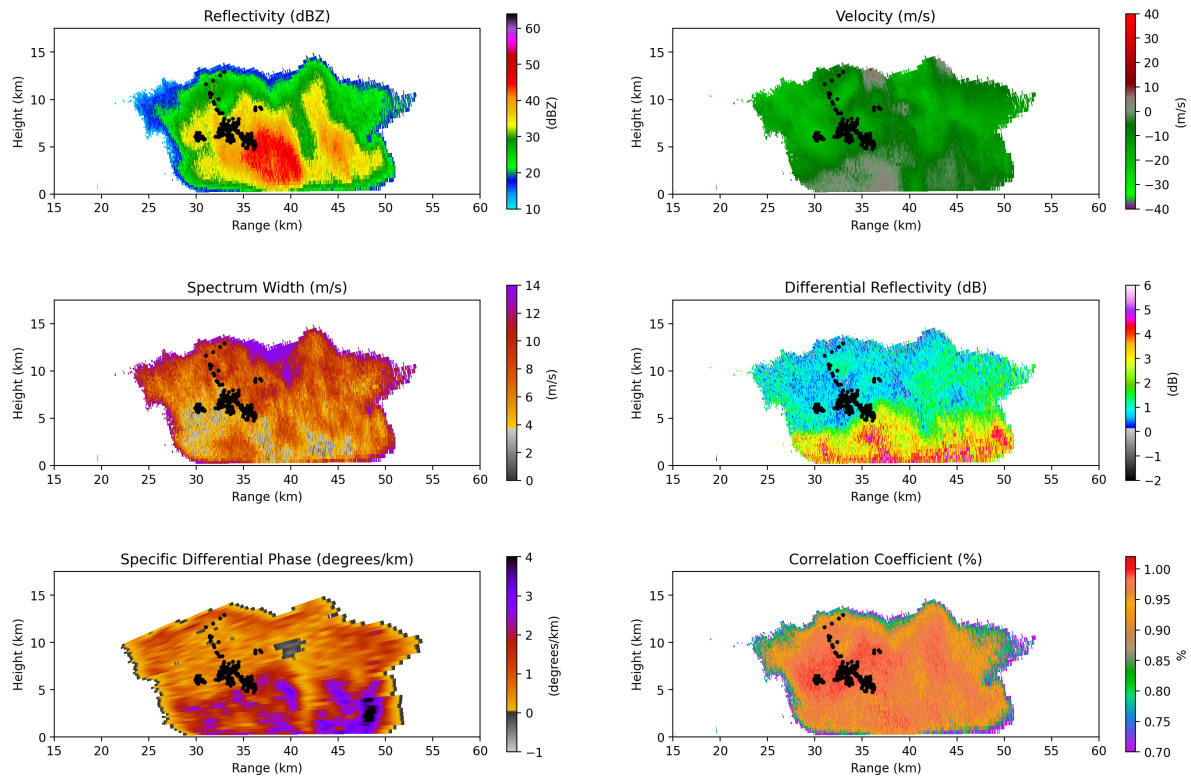


FIG. 3. A Horus RHI scan on 11 May 2023, at 23:38:29 UTC depicting (top left) radar reflectivity (in dBZ), (top right) velocity (in ms⁻¹), (middle left) spectrum width (in ms⁻¹, according to the color scale), (middle right) differential reflectivity (in dB), (bottom left) specific differential phase (in °km⁻¹), and (bottom right) correlation coefficient (in %) during a tornadic supercell embedded in a squall line south of Oklahoma City, Ok. The OKLMA flash sources (black dots) were filtered as described in text. Increasing range is to the west as shown in Fig 1.

are located just below and to the right (west) of the negative K_{DP} signature. This aligns more closely with what Biggerstaff et al. (2017) examined in their study, but the OKLMA data is still only partially in the expected location, and the negative K_{DP} signature is isolated to a single location and not spread out above the updraft. These VHF sources are only around the negative K_{DP} signature for a scan or two before they move away, also. Further into the study period, the negative K_{DP} signature remains isolated with the flashes extending along the entirety of the storm in the RHIs. There are times when the VHF sources occur along the negative K_{DP} signature (Figure 5) and other times when they don't line up at all (Figure 3).

Flash Propagation and Intensity

Flash propagation and intensity in and around the supercell were both well documented by the OKLMA due to the storm's position over the central Oklahoma LMA sites.

Looking at the flash propagations around the RHI scans earlier in the study period, many of the scans had multiple flashes detected within the 3 km range, with many more outside of the range, as well. Figure 6 shows the location of the main flash captured within the 3 km range of the Horus RHI in relation to the overall storm at 23:38:29 UTC. Figure 7 has a more active scan with five different flashes captured in a single RHI. In total, there were 1,311 unique flashes recorded during the 22-minute study period, all of which were within the 3 km sampled volume. Looking at the flash frequency, there was a more active period at the beginning of the period followed by a slight decrease in activity. From 23:38 to 23:45 UTC, flash counts stayed mainly between two to six flashes per RHI scan, then decreased to zero to four flashes during the rest of the period (Figure 8).

HRUS 2023-05-11 23:38:31 UTC

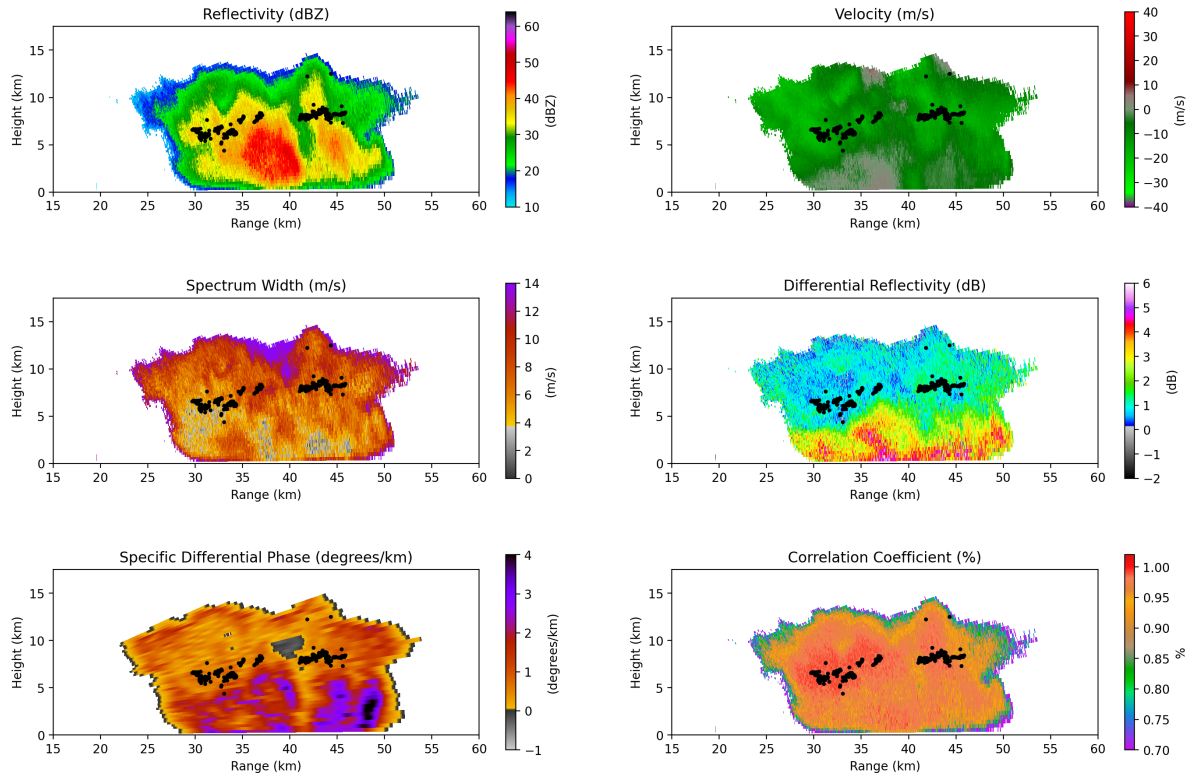


FIG. 4. Same as in Figure 3, but at 23:38:31 UTC, 2 seconds after Figure 3.

4. Discussion and Conclusion

Using Horus's high temporal resolution to analyze ice crystal alignment within thunderstorms was one of the goals of this study. Knowing that Horus can conduct RHI scans in less than two seconds made it plausible to capture ice crystal behaviors within thunderstorms and how the build-up and breakdown of electrical fields affect their orientations. Plotting Horus's RHI scans along with the OKLMA flash source data presented a mixture of findings.

In this study, K_{DP} values did not appear to represent the build-up and breakdown of electric fields. In an ideal case, an electric field should cause K_{DP} values to turn negative as ice crystals begin to vertically orientate, then after the breakdown with lightning channels above and below this volume, go back to a horizontal orientation. However, while a consistent volume of negative K_{DP} was observed by Horus, the flashes observed by the LMA were spread throughout the storm, with little to no change in K_{DP} when any flashes were close to the negative K_{DP} volume. There are some possible reasons why this did not occur during this study:

- Horus's scan times might be too slow to pick up on the repeated build-up and breakdown of electric fields in this case given the large flash rates observed.
- This specific storm may have had too many flashes within it to allow for large volumes of alignment and unalignment of ice crystals in the rapidly changing electric fields.
- Horus is still under development and was undergoing testing at the time. The beam width was wide in the testing setup (about 12 degrees in azimuth and 3.5 degrees in elevation), leading to a larger sample volume in which any more reflective particles may have overwhelmed the signal of any ice crystals present.
- Vulpiani's method for calculating K_{DP} may be off when using the Horus data.

These are just a few possibilities as to why the K_{DP} values did not show the build-up and breakdown of electric fields via vertically orientated ice crystal alignment. Future research will have to be done to investigate each of these

HRUS 2023-05-11 23:39:03 UTC

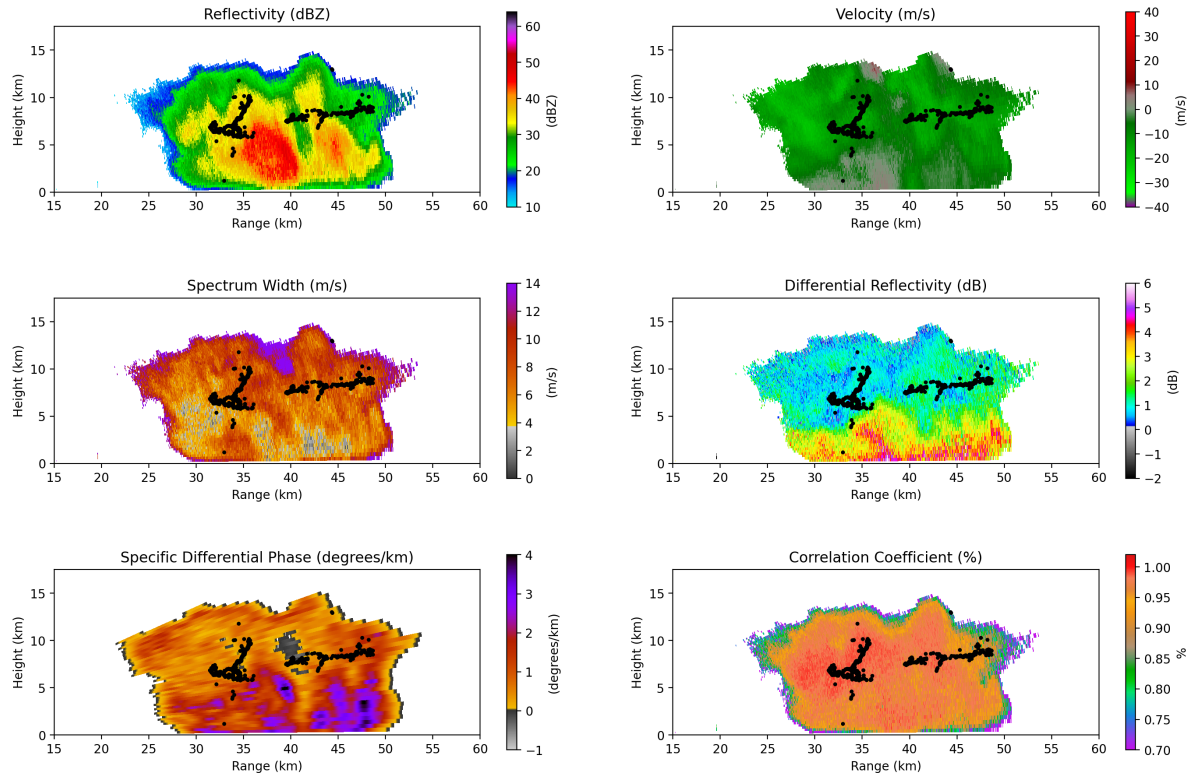


FIG. 5. Same as in Figure 4, but at 23:39:03 UTC, 32 seconds after Figure 3.

potential issues to determine whether they played a factor or not. Even though K_{DP} did not represent the ice crystal alignment process well, Z_{DR} showed some promise in discriminating regions with different microphysical populations favorable for lightning propagation, potentially including ice crystal alignment signatures, as well. Looking at the OKLMA flash source locations compared to the near-zero Z_{DR} locations shows frequent regions of overlap. This leads to the possibility that Z_{DR} values may work as an alternative method for finding radar signatures of electrification and resulting three-dimensional flash locations. This will also require future research to determine how strong of a correlation there is between the two.

The OKLMA data provided us with a very detailed three-dimensional map of the storm's flash propagation and exactly how many flashes were present. This supercell was very electrified with 1,311 flashes recorded within the 3 km RHI scan sampling volumes during the 22-minute study period and 22,351 flashes during the entirety of the scan time. The intensity of the supercell alone may have affected the K_{DP} values, resulting in the lack of electric

field breakdowns and ice crystal unalignment. This study helps to advance our understanding of electrification signatures and how important the spatial and temporal scales are to capturing that process.

Going into this study, the use of radars and LMAs for lighting research has been increasing. In past studies, the use of rapid scanning radars with LMA data had proven successful in capturing electrified regions where ice crystal alignment occurs. What had not been done up to this point, was using a fully digital polarimetric rotating S-band PAR system in conjunction with a LMA system to study ice crystal alignment and storm electrification. Even though this study did not capture the build-up and breakdown of electric fields from ice crystals through K_{DP} signatures, it did manage to bring light to the use of Z_{DR} to potentially determine regions favorable for lightning propagation throughout a thunderstorm. This study showed the high frequency of flashes even with the fast RHI times of Horus. Finally, this study brings forward questions that will need to be addressed in future research. This includes whether the lack of ice crystal alignment was just a

KTLX 23:44:09 UTC 11 May 2023 0.48 deg.

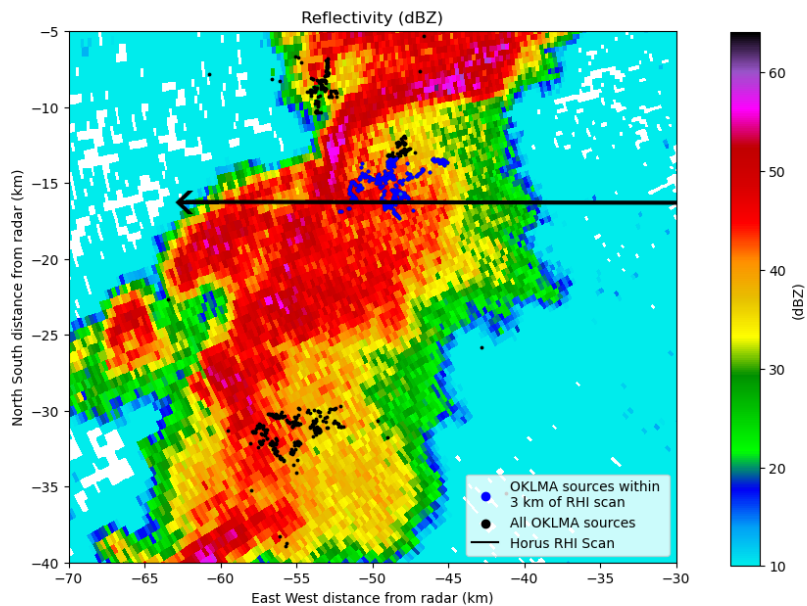


FIG. 6. Base (0.48° elevation) PPI scans of radar reflectivity (dBZ) from the Oklahoma City, OK, WSR-88D radar, KTLX, of a tornadic supercell embedded in a squall line on 11 May 2023 at 23:44:09 UTC. The red square is the location of the mobile PAR, Horus, scanning RHIs at a 270° azimuth angle (black line).

KTLX 23:44:09 UTC 11 May 2023 0.48 deg.

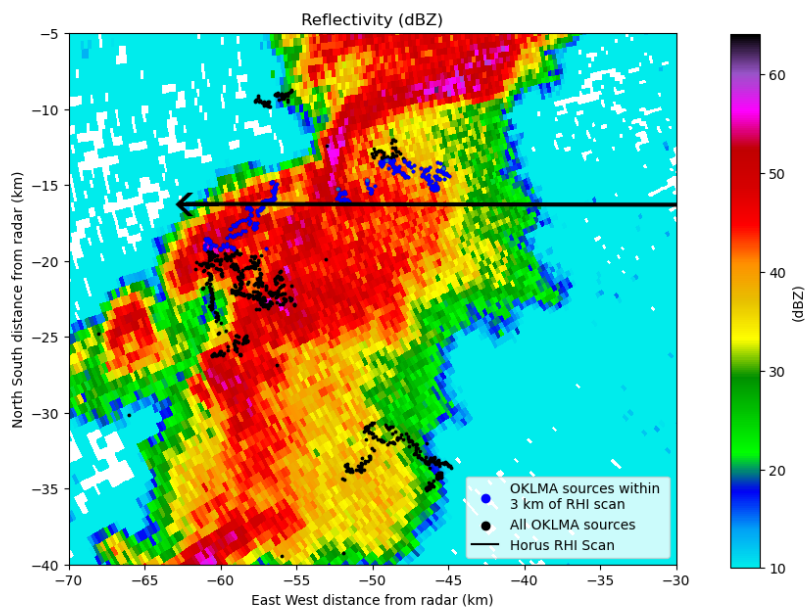


FIG. 7. Same as in Figure 1, but at 23:57:02 UTC, 12 minutes, and 53 seconds after Figure 1.

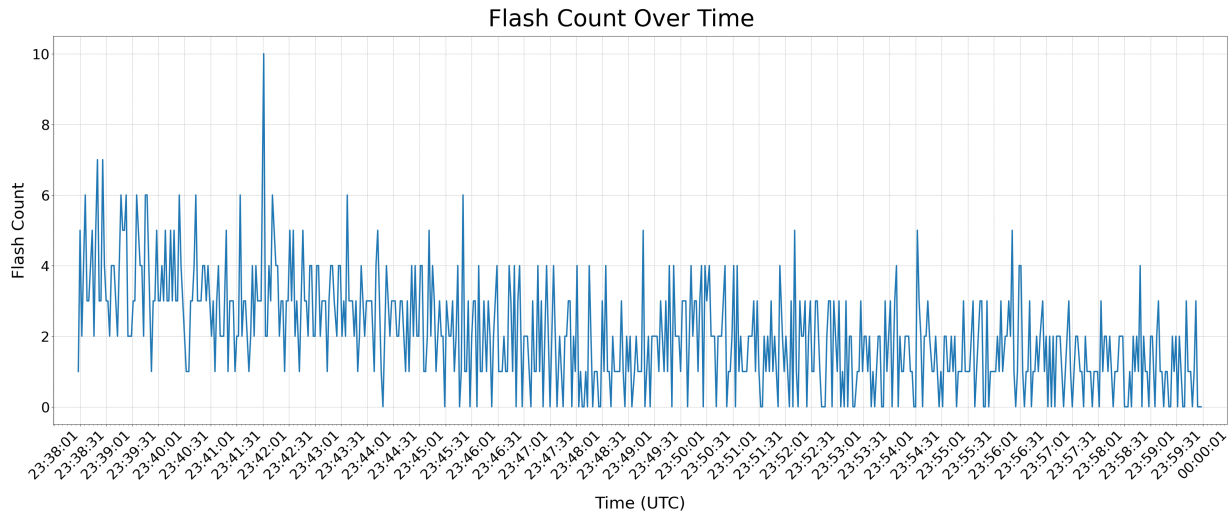


FIG. 8. The number of flashes within the 3 km sampled volume along the Horus RHI scans by the OKLMA during the period from 11 May 2023 at 23:38 to 12 May 2023 at 00:00 UTC. The number of flashes recorded is along the y-axis and the time (UTC) it occurred is along the x-axis which corresponds to the 2-second RHI scans that were conducted by Horus. There were a total of 1,311 flashes recorded along the RHI scans, within the 3 km sampling area, during this period.

temporal limitation of the radar scans, a limitation of the large sampling volume and the mixture of particles present within them, or the lack of physical time for crystals to align and stay aligned due to high flash rates. This study is the beginning of a large project that will hope to provide some insight into the lightning and storm electrification processes that occur within thunderstorms and advance our understanding moving forward.

Acknowledgments. This material is based upon work supported by the National Science Foundation under Grant No. AGS-2050267 and Grant No. 2310336. The authors would like to thank Dr. Daphne LaDue and Alex Marmo for running a fantastic program and creating an environment in which the career path of a research scientist can be explored. Extended thanks are given to the National Weather Center (NWC), the Advanced Radar Research Center (ACCR), and the University of Oklahoma (OU) for being a part of this REU. Lastly, Cory would like to specifically thank Dr. David Schwartzman, Dr. Vanna Chmielewski, Dr. David Bodine, Dr. Tian-You Yu, and Dr. Michael Stock, for their amazing mentorship during the course of this summer. The statements, findings, conclusions and recommendations in this study do not necessarily reflect the views of the University of Oklahoma (OU), the National Weather Center (NWC), or other NOAA affiliates.

References

- Barth, M. C., and Coauthors, 2015: The deep convective clouds and chemistry (DC3) field campaign. **96** (8), 1281–1309, doi:10.1175/BAMS-D-13-00290.1, URL <https://journals.ametsoc.org/view/journals/bams/96/8/bams-d-13-00290.1.xml>, publisher: American Meteorological Society Section: Bulletin of the American Meteorological Society.
- Biggerstaff, M. I., Z. Zounes, A. Addison Alford, G. D. Carrie, J. T. Pilkey, M. A. Uman, and D. M. Jordan, 2017: Flash propagation and inferred charge structure relative to radar-observed ice alignment signatures in a small florida mesoscale convective system. **44** (15), 8027–8036, doi:10.1002/2017GL074610, URL <https://onlinelibrary.wiley.com/doi/abs/10.1002/2017GL074610>, eprint: <https://onlinelibrary.wiley.com/doi/pdf/10.1002/2017GL074610>.
- Chmielewski, V. C., and E. C. Bruning, 2016: Lightning mapping array flash detection performance with variable receiver thresholds. **121** (14), 8600–8614, doi:10.1002/2016JD025159, URL <https://onlinelibrary.wiley.com/doi/abs/10.1002/2016JD025159>, eprint: <https://onlinelibrary.wiley.com/doi/pdf/10.1002/2016JD025159>.
- Feng, Z., X. Dong, and B. Xi, 2009: A method to merge WSR-88d data with ARM SGP millimeter cloud radar data by studying deep convective systems. **26** (5), 958–971, doi:10.1175/2008JTECHA1190.1, URL <https://journals.ametsoc.org/view/journals/atos/26/5/2008jtecha1190.1.xml>, publisher: American Meteorological Society Section: Journal of Atmospheric and Oceanic Technology.
- Fuchs, B. R., E. C. Bruning, S. A. Rutledge, L. D. Carey, P. R. Krehbiel, and W. Rison, 2016: Climatological analyses of LMA data with an open-source lightning flash-clustering algorithm. **121** (14), 8625–8648, doi:10.1002/2015JD024663, URL <https://onlinelibrary.wiley.com/doi/abs/10.1002/2015JD024663>, eprint: <https://onlinelibrary.wiley.com/doi/pdf/10.1002/2015JD024663>.
- Haupt, R. L., and Y. Rahmat-Samii, 2015: Antenna array developments: A perspective on the past, present and future. **57** (1), 86–96, doi:10.1109/MAP.2015.2397154, conference Name: IEEE Antennas and Propagation Magazine.
- Helmus, J. J., and S. M. Collis, 2016: The python ARM radar toolkit (py-ART), a library for working with weather radar data

- in the python programming language. **4** (1), e25, doi:10.5334/jors.119, URL <https://openresearchsoftware.metajnl.com/articles/10.5334/jors.119>, number: 1 Publisher: Ubiquity Press.
- Hendry, A., and Y. M. M. Antar, 1982: Radar observations of polarization characteristics and lightning-induced realignment of atmospheric ice crystals. **17** (5), 1243–1250, doi:10.1029/RS017i005p01243, URL <https://onlinelibrary.wiley.com/doi/abs/10.1029/RS017i005p01243>, eprint: <https://onlinelibrary.wiley.com/doi/pdf/10.1029/RS017i005p01243>.
- Hubbert, J. C., S. M. Ellis, W.-Y. Chang, and Y.-C. Liou, 2014: X-band polarimetric observations of cross coupling in the ice phase of convective storms in taiwan. **53** (6), 1678–1695, doi:10.1175/JAMC-D-13-0360.1, URL <https://journals.ametsoc.org/view/journals/apme/53/6/jamc-d-13-0360.1.xml>, publisher: American Meteorological Society Section: Journal of Applied Meteorology and Climatology.
- Kumjian, M., 2013: Principles and applications of dual-polarization weather radar. part III: Artifacts. **1** (21), 265–274, doi:10.15191/nwajom.2013.0121, URL <http://nwafiles.nwas.org/jom/articles/2013/2013-JOM21/2013-JOM21.pdf>.
- MacGorman, D. R., and Coauthors, 2008: TELEX the thunderstorm electrification and lightning experiment. **89** (7), 997–1014, doi:10.1175/2007BAMS2352.1, URL <https://journals.ametsoc.org/view/journals/bams/89/7/2007bams2352.1.xml>, publisher: American Meteorological Society Section: Bulletin of the American Meteorological Society.
- Maese, T., J. Melody, S. Katz, M. Olster, W. Sabin, A. Freedman, and H. Owen, 2001: Dual-use shipborne phased array radar technology and tactical environmental sensing. *Proceedings of the 2001 IEEE Radar Conference (Cat. No.01CH37200)*, 7–12, doi:10.1109/NRC.2001.922942.
- Maggio, C., and Coauthors, 2005: Lightning-initiation locations as a remote sensing tool of large thunderstorm electric field vectors. **22** (7), 1059–1068, doi:10.1175/JTECH1750.1, URL <https://journals.ametsoc.org/view/journals/atot/22/7/jtech1750.1.xml>, publisher: American Meteorological Society Section: Journal of Atmospheric and Oceanic Technology.
- Palmer, R. D., and Coauthors, 2023: Horus—a fully digital polarimetric phased array radar for next-generation weather observations. **1**, 96–117, doi:10.1109/TRS.2023.3280033, conference Name: IEEE Transactions on Radar Systems.
- Rison, W., R. J. Thomas, P. R. Krehbiel, T. Hamlin, and J. Harlin, 1999: A GPS-based three-dimensional lightning mapping system: Initial observations in central new mexico. **26** (23), 3573–3576, doi:10.1029/1999GL010856, URL <https://onlinelibrary.wiley.com/doi/abs/10.1029/1999GL010856>, eprint: <https://onlinelibrary.wiley.com/doi/pdf/10.1029/1999GL010856>.
- Stough, S. M., L. D. Carey, C. J. Schultz, and D. J. Cecil, 2022: Supercell thunderstorm charge structure variability and influences on spatial lightning flash relationships with the updraft. **150** (4), 843–861, doi:10.1175/MWR-D-21-0071.1, URL <https://journals.ametsoc.org/view/journals/mwre/150/4/MWR-D-21-0071.1.xml>, publisher: American Meteorological Society Section: Monthly Weather Review.
- Sullivan, A. W., and J. D. Wells, 1957: A lightning stroke counter. **38** (5), 291–294, doi:10.1175/1520-0477-38.5.291, URL <https://journals.ametsoc.org/view/journals/bams/38/5/1520-0477-38.5.291.xml>, ISBN: 9781520047737 Publisher: American Meteorological Society Section: Bulletin of the American Meteorological Society.
- Takahashi, T., 1978: Riming electrification as a charge generation mechanism in thunderstorms. **35** (8), 1536–1548, doi:10.1175/1520-0469(1978)035<1536:REAACG>2.0.CO;2, URL https://journals.ametsoc.org/view/journals/atsc/35/8/1520-0469_1978_035_1536_reaacg_2.0.co_2.xml, publisher: American Meteorological Society Section: Journal of the Atmospheric Sciences.
- Thomas, R. J., P. R. Krehbiel, W. Rison, S. J. Hunyady, W. P. Winn, T. Hamlin, and J. Harlin, 2004: Accuracy of the lightning mapping array. **109**, doi:10.1029/2004JD004549, URL <https://onlinelibrary.wiley.com/doi/abs/10.1029/2004JD004549>, eprint: <https://onlinelibrary.wiley.com/doi/pdf/10.1029/2004JD004549>.
- Vulpiani, G., M. Montopoli, L. D. Passeri, A. G. Gioia, P. Giordano, and F. S. Marzano, 2012: On the use of dual-polarized c-band radar for operational rainfall retrieval in mountainous areas. **51** (2), 405–425, doi:10.1175/JAMC-D-10-05024.1, URL <https://journals.ametsoc.org/view/journals/apme/51/2/jamc-d-10-05024.1.xml>, publisher: American Meteorological Society Section: Journal of Applied Meteorology and Climatology.
- Zikmunda, J., and G. Vali, 1972: Fall patterns and fall velocities of rimed ice crystals. **29** (7), 1334–1347, doi:10.1175/1520-0469(1972)029<1334:FPAFVO>2.0.CO;2, URL https://journals.ametsoc.org/view/journals/atsc/29/7/1520-0469_1972_029_1334_fpafvo_2.0.co_2.xml, publisher: American Meteorological Society Section: Journal of the Atmospheric Sciences.